Eur Biophys J (2011) 40:1115–1120
DOI 10.1007/s00249-011-0738-8

ORIGINAL PAPER

Use of EPR and FTIR to detect biological effects of ultrasound and microbubbles on a fibroblast cell line

D. Pozzi · P. Fattibene · D. Viscomi · L. Di Giambattista · P. Grimaldi · I. Udroiu · A. Bedini · C. Giliberti · R. Palomba · A. Congiu Castellano

Received: 2 March 2011 / Revised: 6 July 2011 / Accepted: 19 July 2011 / Published online: 25 August 2011

Abstract Structural and functional effects of exposing murine fibroblasts (NIH 3T3) to therapeutic ultrasound at 1 MHz frequency are described. These bioeffects can be attributed to the formation of free radical species by sonolysis of water. When cavitation occurs, dissociation of water vapor into H atoms and OH radicals is observed; these H atoms and OH radicals combine to form H_2, H_2O_2, and HO_2. The radicals can chemically modify biomolecules, for example enzymes, DNA, and lipids. Generation of free radicals during exposure to ultrasound with or without encapsulated microbubbles (contrast agents) was studied by use of electron paramagnetic resonance with DMPO spin trapping. Recently the potential for possible use of these microbubbles in gene therapy has been investigated, because of the ability of the stabilized microbubbles to release their content when exposed to ultrasound. Structural changes were studied by Fourier-transform infrared spectroscopy, and induction of possible genotoxic damage by exposure of the cells to therapeutic ultrasound at 1 MHz frequency with our experimental device was verified by use of the cytokinesis-block micronucleus assay.

Keywords Therapeutic ultrasound · Free radicals · EPR spectroscopy · FTIR spectroscopy · CBMN assay · Contrast agents

Special Issue: SIBPA 2011 Meeting.

D. Pozzi (✉)
Experimental Medicine Department, Sapienza,
University of Rome, V.le Regina Elena, 324, 00161 Rome, Italy
e-mail: deleana.pozzi@uniroma1.it

P. Fattibene · D. Viscomi
ISS, V.le Regina Elena, 299, 00161 Rome, Italy

L. Di Giambattista · P. Grimaldi · A. Congiu Castellano
Physics Department, Sapienza, University of Rome,
P. le A. Moro, 2, 00185 Rome, Italy

L. Di Giambattista
CISB (Interdepartmental Research Centre for Biomedical Systems Models and Information Analysis), Rome, Italy

I. Udroiu · A. Bedini · C. Giliberti · R. Palomba
DIPIA, INAIL/ISPESL, via Urbana 167, Rome, Italy

Introduction

There are two main reasons for study of the effects of ultrasound on cell lines. Photodynamic therapy (PDT) is an alternative therapy for treating deceases related to the generation of reactive oxygen species (ROS) during light-activated photosensitizer treatment (Yow et al. 2007; Xiang et al. 2010; Wang et al. 2010). However, because of the poor penetration of biological tissues by light, PDT is limited to treatment of surface tumors. Recent studies have shown that ultrasound waves can effectively activate photosensitizers, inducing intracellular accumulation of ROS, resulting in the death of tumor cells (Kuroki et al. 2007; Rosenthal et al. 2004; Hiraoka et al. 2006). Because ultrasound penetrates biological tissues more effectively than photons, sonodynamic therapy (SDT) provides new ways for application of ultrasound waves in cancer treatment.

Free radical formation is a direct result of sonolysis of water in the presence of a monoatomic gas (Barnett 1998; Strom-Jensen and Dunn 1984). When cavitation occurs in response to the passage of ultrasonic waves through water, dissociation of water vapor into H^+ atoms and $^{\cdot}OH^-$ radicals is observed. The H^+ atoms and $^{\cdot}OH^-$ radicals either combine to form H_2, H_2O_2, and HO_2, or the radicals can

chemically modify biomolecules, for example enzymes, DNA, and lipids.

Ultrasound also has potential for improving the efficiency of gene delivery into tissues and cells, a technique known as sonophoresis/sonoporation. It is known that cell membranes constitute one of the greatest barriers to delivery of drugs, proteins, DNA, and other molecules into cells and tissues. The ability of ultrasound to transiently disrupt these barriers in living cells, causing transient pores to open in the membrane, could provide an important tool for delivery of macromolecular drugs or other compounds requiring access to the cytosol (Shohet et al. 2000; Christiansen et al. 2003; Bekeredjian et al. 2003). In addition, it has been reported that microbubbles, used as ultrasound contrast agents, enhance the efficiency of gene delivery without causing cell damage. In general, cell damage depends on ultrasound intensity, concentration of microbubbles, and cell type. Especially, ultrasound intensity and exposure time are key factors. Therefore, it is important to optimize the ultrasound exposure conditions during ultrasound-mediated gene delivery.

Contradictory results concerning the cellular damage induced by ultrasound prompted us to focus our attention on the effects of therapeutic ultrasound (1 MHz frequency) on a healthy cell line, murine fibroblasts (NIH-3T3 cells), by considering the generation of free radicals. The objective of the work reported in this paper was, therefore, to find a correlation between possible membrane damage and the free radicals induced by ultrasound. By use of FTIR–ATR spectroscopy in the 3,000–2,800 cm^{-1} region, which is the lipid fingerprint region, structural changes of sonicated cells can be detected. By use of EPR measurements in spin-trapping mode the free radicals produced during exposure can be evaluated. In this work, the free radical intermediates ($^{\cdot}OH^{-}$) formed during ultrasound exposure in phosphate-buffered saline were evaluated by use of the nitrone spin trap 5,5-dimethyl-1-pyrroline-*N*-oxide (DMPO). Genotoxic damage of cells exposed to ultrasound was monitored by use of the cytokinesis-block micronucleus (CBMN) assay.

Materials and methods

Cells and culture conditions

The experiments were conducted on a healthy adherent murine fibroblast cell line, NIH-3T3 cells. These cells were incubated at 37°C, in a 5% CO_2 humidified atmosphere, in a solution of Dulbecco's modified Eagle's medium (DMEM) supplemented with 10% fetal bovine serum (FBS), 1% penicillin, and 1% L-glutamine/streptomycin. Concentration and cell vitality of both the untreated (control) and the US-treated (sonicated) cells was determined by use of the trypan blue (TB) exclusion test. For our experiments, sample vitality, before US exposure, was better than 90% for each trial. Cell vitality after maximum exposure time (60 min) to ultrasound was approximately 70% for NIH-3T3 cells. The experiment was performed in triplicate.

Microbubbles

SonoVue® microbubbles (Bracco, Milan, Italy) were reconstituted in saline solution (2.5×10^8 microbubbles/ml); the average diameter of these bubbles was 2.5–6 μm. An aliquot (10 μl) of this suspension was added to 10 ml Dulbecco's phosphate buffer solution (PBS) in a Petri dish at the beginning of the experiment (Wang et al. 2009).

SonoVue® microbubbles are an example of an important family of microbubbles whose membrane consists of phospholipids filled with sulfur hexafluoride (SF6), a gas with low solubility. In particular, the SonoVue microbubbles, because of the high flexibility of their shell, are strongly echogenic over a wide range of frequencies and acoustic pressure and can, therefore, be used with both destructive and conservative contrast bubble-specific imaging methods.

Ultrasound exposure

Ultrasound was applied using settings described elsewhere and able to produce reactive oxygen species (Juffermans et al. 2006; Marchioni et al. 2009). The ultrasound apparatus was a conventional physiotherapy device (provided by ISPESL, Italy) with a resonant frequency of 1 MHz. The apparatus works in the range from 10 to 100% of maximum power emitted with a signal duty cycle variable. The US field measurements were made using a needle hydrophone of 1 mm diameter (S.N.1470) with a sensitivity of 1,670.4 mV/MPa at 1 MHz, produced and calibrated by Precision Acoustics (Higher Bockhampton, Dorchester, DT2 8QH, UK). Preliminary tests enabled choice of suitable sonication conditions and the setup maximum power in pulsed mode with the 75% duty cycle. The ultrasonic transducer, whose active part has circular geometry of 3 cm diameter, was placed at the bath surface of a tank filled with partially degassed water at a controlled temperature of 25°C. As shown in Fig. 1, the Petri dish, filled with cell culture, and whose surface was 9.6 cm^2, was placed on the bottom of the tank, aligned with the transducer at 3 cm distance. The measured pulsed average intensity, I_{PA}, was 0.038 ± 0.002 W cm^{-2}. The temperature inside and outside the Petri dish during ultrasound exposure was monitored by use of a thermocouple; we found the temperature rise (<2°C) inside the Petri dish to be unlikely to induce thermal damage to the cells. The sonication time was 30 min.

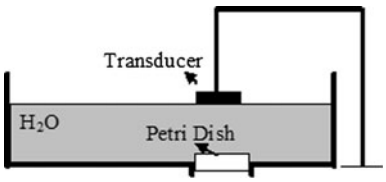

Fig. 1 The experimental setup of the ultrasonic exposure

FTIR spectroscopy

Spectra were recorded in the 900–3,000 cm^{-1} region by use of a Jasco FTIR/410 spectrometer equipped with a conductive ceramic coil mounted in a water-cooled copper jacket source, a KBr beamsplitter, and a standard TGS detector.

The NIH-3T3 cell spectra were acquired in transmission mode; cells were cultured on an infrared-transparent CaF_2 window previously treated with polylysine to promote cell attachment and placed in Petri dishes. The cellular monolayer adhering to the CaF_2 window was sonicated, washed in PBS, and dried in a desiccator; for each spectrum, a resolution of 4 cm^{-1} was used, and 64 interferograms were coadded and apodized with a triangular function (Pozzi et al. 2007; Di Giambattista et al. 2010).

Preliminary reduction of IR spectral data (subtraction, smoothing, etc.) was performed by use of Jasco Spectra Manager and Origin Pro 8.0 software. By comparing the second derivative of the spectra, the most significant regions were found and confirmed by use of a non-parametric statistical test, the Kruskal–Wallis test (Di Giambattista et al. 2011), on all corrected underived spectra (level of significance $P = 0.05$; data not reported).

Finally, FTIR results from sonication with and without microbubbles and from control samples were analyzed by one-way analysis of variance ANOVA (significance level $P < 0.05$); moreover, the means of these FTIR results were checked by use of a Tukey means comparison method.

Electron paramagnetic resonance (EPR) spin trapping for detection of free-radical formation

5,5-Dimethyl-1-pyrroline-*N*-oxide (DMPO; high-purity; Alexis Biochemicals) was used as spin-trap reagent. The concentrations of DMPO were determined spectrophotometrically ($\varepsilon_{234} = 7.7 \times 10^3$ mol^{-1} dm^3 cm^{-1}). A solution of DMPO (150 mM) was added to the samples before the start of sonication. At the end of the sonication time (30 min), an aliquot from the supernatant of the sample was transferred immediately to capillary tubes held inside flat-bottomed Suprasil tubes and spectrum acquisition was started within 5 min after the end of the sonication. Unsonicated samples (sham controls) where stored for 35 min before EPR measurements, under the same experimental conditions of the sonicated samples.

A Bruker Elexsys E500 cw spectrometer operating in the X band and equipped with an SHQ cavity was used for EPR measurements. Sample preparation and EPR measurements were performed in a laboratory under controlled conditions of temperature (22 ± 1°C) and relative humidity (48 ± 1%). The position of the sample tube inside the cavity was reproducible in height and angular orientation.

The two central lines of the typical DMPO-OH 1:2:2:1 quartet spectrum were detected using the settings: modulation frequency, 100 kHz; microwave frequency, 9.84 GHz; sweep field, 2.5 mT; time constant, 163 ms; conversion time, 41 ms; number of averaging scans 20. EPR spectra were recorded at modulation amplitude of 0.07 mT and a microwave power of 8 mW. The microwave frequency was monitored on an external frequency counter (HP53150A). In order to investigate the relative amounts of radicals in the DMPO solutions, the peak-to-peak amplitude of the second line of the DMPO-OH 1:2:2:1 quartet spectrum was measured. Because of the high reproducibility of the experimental set up, relative changes in signal intensities were related to relative changes in free radical concentration. No efforts were made to convert the signal intensity to absolute concentration because it was considered irrelevant to this study. In every measurement session the sonicated and unsonicated cells with and without the SonoVue® microbubbles were studied; each experimental session did not exceed 12 h and measurements were repeated three times. The experimental data were analyzed by one-way ANOVA (significance level $P < 0.05$).

Cytokinesis-block micronucleus (CBMN) assay

Control and sonicated cellular samples were treated with 6 μg/ml cytochalasin B. The cells were collected 24 h after addition of cytochalasin B, by centrifugation for 5 min, then carefully resuspended in 5 ml hypotonic saline (75 mM KCl). Immediately after addition of the hypotonic solution, the cells were collected and fixed in Carnoy's fixative (3:1 methanol–acetic acid). Finally, samples of the cells were transferred on to pre-cleaned slides and stained with 10 μg/ml 4′,6′-diamidino-2-phenylindole (DAPI) in antifade solution (Vector Laboratories). By use of a Zeiss Axiophot microscope with ultraviolet light (359 nm excitation filter, 441 nm barrier filter) small cytoplasmatic bodies, named micronuclei (MN_I), also known as Howell–Jolly bodies, were scored. A micronucleus (MN) is formed during the metaphase/anaphase transition of mitosis (cell division). It may arise from a whole lagging chromosome (aneugenic event leading to chromosome loss) or from an acentric chromosome fragment becoming detached from a chromosome after breakage (clastogenic event) which is

not integrated into the daughter nuclei (Kirsch-Volders and Fenech 2001). The samples were coadded and scored blind by the same analyst. From each sample, 500 total cells were scored in order to evaluate the nuclear division index (NDI).

This index, an indicator of possible mutagenic and cytotoxic effects of the US, was evaluated for each sample by use of the equation:

$$\mathrm{NDI} = \frac{(\mathrm{Mono} + 2\mathrm{BNC} + 3\mathrm{TNC} + 4\mathrm{QNC})}{(\mathrm{Mono} + \mathrm{BNC} + \mathrm{TNC} + \mathrm{QNC})}$$

where Mono, BNC, TNC, and QNC, respectively, indicate the number of mono, bi, tri, and quadri-nucleate cells.

Results and discussion

EPR spectroscopy

Four EPR spectra of DMPO-OH adducts from unsonicated and sonicated cells with and without SonoVue® are reported in Fig. 2a. Each spectrum is the average of spectra from two samples of the same suspension, measured in two sessions. A difference is evident between the spectrum intensity of sonicated and unsonicated cells, whereas the presence of SonoVue® seemed not to cause any difference. The quantitative analysis of this result given in Fig. 2b shows the mean value and the minimum–maximum deviation of the peak-to-peak amplitude of the two spectra measured in the two sessions: the 1 MHz ultrasound exposure is responsible for a statistically significant increase (as obtained by one-way ANOVA with $P < 0.05$ as the level of significance; data not shown) of the quantity of free radicals. By contrast the spectra of the cells in the presence or absence of SonoVue® microbubbles were not statistically significantly different.

FTIR spectroscopy

As reported in our a previous work (Marchioni et al. 2009; Di Giambattista et al. 2009; Conti et al. 2010), ATR-FTIR spectroscopy can be used to detect whether therapeutic ultrasound has reversible or irreversible effects on cells, and the dependence of these effects on exposure geometry and energy dose. Our results also demonstrated that ATR-FTIR spectroscopy can be used to identify biological effects at energy doses lower than those required to induce toxicity such as revealed by conventional cell-biology assays (Conti et al. 2010). IR spectroscopic markers could, therefore, be used to reveal cellular damage caused by ultrasound at low energy doses.

A significant change in the FTIR spectra of the samples was observed in the frequency region between 3,000 and 2,800 cm^{-1}, named the lipid region; the IR spectra obtained in this region from sham control cells and from cells sonicated (30 min) with or without the SonoVue® are compared in Fig. 3.

The bands at 2,958 and 2,924 cm^{-1} arise from the asymmetric stretching vibration modes of CH_2, indicated $\nu_{as}(CH_2)$, and CH_3, indicated $\nu_{as}(CH_3)$, respectively (Draux et al. 2009; Gasper et al. 2009). Their intensity absorption ratio $\left(I_{\mathrm{ratio}} = \frac{I_1(CH_2)_{as}}{I_2(CH_3)_{as}}\right)$ decreases when the cells are under hypoxia or low glucose concentrations, reflecting a per-oxidative state of the cell membrane phospholipids. As observed in Fig. 3, our FTIR results show that this ratio decreases under sonication conditions and, mainly, in the presence of the SonoVue® microbubbles. The other

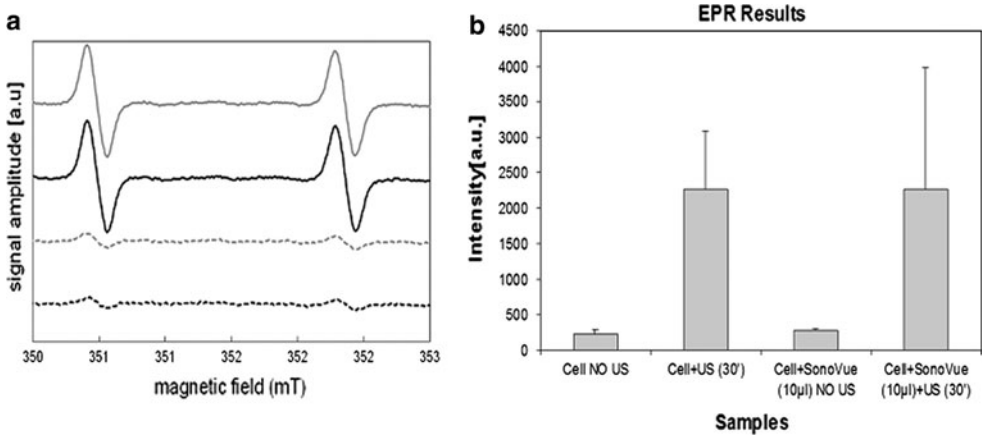

Fig. 2 **a** EPR spectra of the DMPO-OH adducts of unsonicated and 1 MHz-sonicated cells with and without SonoVue® microbubbles in phosphate-buffered saline. *From bottom to top*: control cells (unsonicated and without microbubbles); control cells with 10 µl SonoVue®; sonicated cells, no microbubbles; sonicated cells with 10 µl SonoVue®. **b** Mean value of the peak-to-peak amplitude of the two spectra measured in the two sessions for the four cell samples. The *error bar* is the minimum–maximum deviation

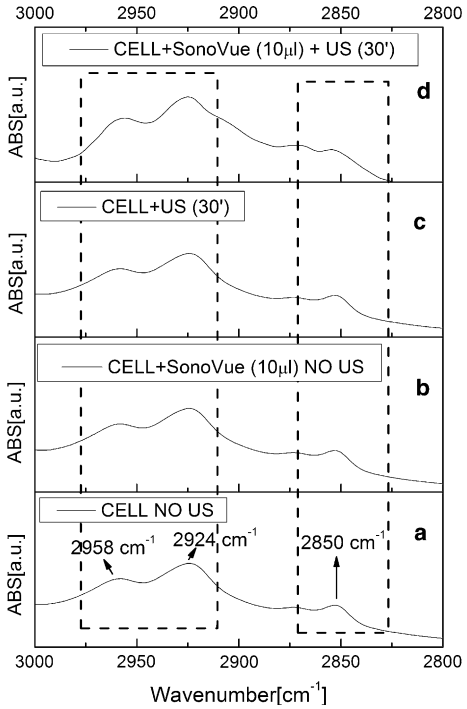

Fig. 3 The regions indicated by *dotted lines* show the absorption peaks at 2,924, 2,958, and 2,850 cm^{-1} for **a** unsonicated control samples, **b** unsonicated with SonoVue, **c** sonicated 30 min, **d** sonicated 30 min with SonoVue

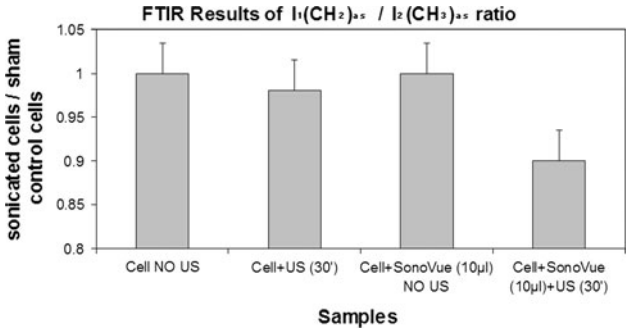

Fig. 4 Intensity absorption ratio, I_{ratio}, normalized to the sham control, is reported for: unsonicated cells (*Cell NO US*), sonicated cells (*cell + US*), unsonicated cells with SonoVue (*Cell + SonoVue NO US*), and sonicated cells with SonoVue (*Cell + SonoVue + US*)

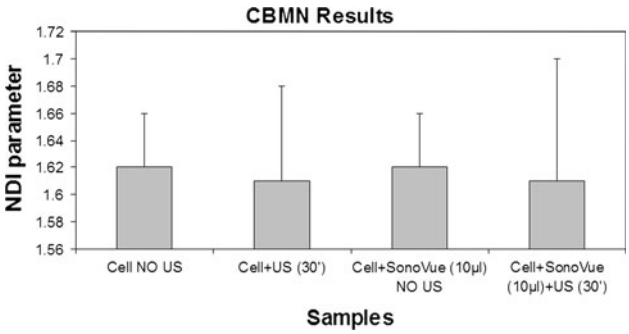

Fig. 5 NDI calculated for unsonicated and sonicated cells without and with SonoVue microbubbles

spectroscopic band at 2,850 cm^{-1} is assigned to the CH_2 symmetric stretching mode which is directly related to the lipid acyl, mainly saturated, chains and this feature is selected as a marker for lipid concentration. As shown in Fig. 3, the frequency of this band is conformation-sensitive and responds to the ultrasound-induced changes in acyl chains, especially when the contrast agent is used. Therefore, the combination of these exposure conditions and observed effects in the lipid region can modify the mechanism of permeabilization of the cell membrane. These differences between sonicated cells with or without the bubbles and sham controls are statistically significant, as assessed by one-way ANOVA (data not shown). Moreover, comparison of the means by use of the Tukey test shows that the difference between the means is significant between the sonicated samples with SonoVue® and the corresponding control, and between the sonicated samples with and without SonoVue® (Fig. 4).

The cytogenetic test

The last question, whether the structural changes revealed by FTIR spectroscopy are connected with a genotoxic effect, can be resolved by study of the MN_I frequency (data not shown) and of the complementary nuclear division index (NDI) for the cellular samples, as reported in Fig. 5.

Our results show that under these experimental conditions there is no significant cytotoxic effect of ultrasound exposure, even in the presence of microbubbles.

Conclusions

As reported in Fig. 2b, exposure to a 1 MHz ultrasound source for 30 min leads to a statistically significant increase of the quantity of free radicals which is the same in presence or absence of SonoVue® microbubbles. This increase in free radicals can alter the cellular equilibrium, inducing peroxidative stress on cellular components, for example the phospholipidic component of the plasma membrane.

The spectroscopic property intensity absorption ratio, I_{ratio}, which is sensitive to variation of cellular peroxidative state, is lower for sonicated samples than for unsonicated samples when the amount of free radical increases; at the plasma membrane level the decrease of the intensity absorption ratio, which is more evident if microbubbles are present, is related to structural changes induced by the free radicals and amplified in the presence of the microbubbles,

as shown in Fig. 3 and described elsewhere (Wang et al. 2009).

Contrast agents are not important in the production of free radicals during sonication, but can amplify the biological effects on the plasma membrane. On the other hand the non-significant differences in the value of NDI for unexposed cells and cells exposed to US show that the energy dose during sonication at 1 MHz is too low to induce toxic effects. Therefore, our experimental set up and ultrasound conditions enable modification of cell membrane permeability without inducing cell death.

References

Barnett S (1998) Free radical production: its biological consequences. Ultrasound Med Biol 24(Suppl 1):S29–S34

Bekeredjian R, Chen S, Frenkel PA, Grayburn PA, Shohet RV (2003) Ultrasound-targeted microbubble destruction can repeatedly direct highly specific plasmid expression to the heart. Circulation 108:1022–1026

Christiansen JP, French BA, Klibanov AL, Kaul S, Lindner JR (2003) Targeted tissue transfection with ultrasound destruction of plasmid-bearing cationic microbubbles. Ultrasound Med Biol 29:1759–1767

Conti L, Grimaldi P, Udroiu I, Bedini A, Giliberti C, Giuliani L, Palomba R, Congiu Castellano A (2010) Effects induced in cells by ultrasound revealed by ATR-FTIR spectroscopy. Vib Spectrosc 52:79–84

Di Giambattista L, Grimaldi P, Udroiu I, Pozzi D, Cinque G, Frogley M, Giansanti A, Congiu Castellano A (2009) FTIR spectral imaging as a probe of ultrasound effect on cells in vitro. Biophys Bioeng Lett 2:2

Di Giambattista L, Grimaldi P, Gaudenzi S, Pozzi D, Grandi M, Morrone S, Silvestri I, Congiu Castellano A (2010) UVB radiation induced effects on cells studied by FTIR spectroscopy. Eur Biophys J 39:929

Di Giambattista L, Pozzi D, Grimaldi P, Gaudenzi S, Morrone S, Congiu Castellano A (2011) New marker of tumor cell death revealed by ATR-FTIR spectroscopy. Anal Bioanal Chem 399(8):2771–2778. doi:10.1007/s00216-011-4654-7

Draux F, Jeannesson P, Gobinet C, Sule-Suso J, Pijanka J, Sandt C, Dumas P, Manfait M, Sockalingum GD (2009) IR spectroscopy reveals effect of non-cytotoxic doses of anti-tumour drug on cancer cells. Anal Bioanal Chem 395:2293–2301

Gasper R, Dewelle J, Kiss R, Mijatovic T, Goormaghtigh E (2009) IR spectroscopy as a new tool for evidencing antitumor drug signatures. Biochim Biophys Acta 1788:1263–1270

Hiraoka W, Honda H, Feril LB Jr, Kudo N, Kondo T (2006) Comparison between sonodynamic effect and photodynamic effect with photosensitizers on free radical formation and cell killing. Ultrasound Sonochem 13:535–542

Juffermans LJM, Dijkmans PA, Musters RJP, Visser CA, Kamp O (2006) Transient permeabilization of cell membranes by ultrasound-exposed microbubbles is related to formation of hydrogen peroxide. Am J Physiol Heart Circ Physiol 291:H1595–H1601

Kirsch-Volders M, Fenech M (2001) Inclusion of micronuclei in non-divided mononuclear lymphocytes and necrosis/apoptosis may provide a more comprehensive cytokinesis block micronucleus assay for biomonitoring purposes. Mutagenesis 16:51–58

Kuroki M, Hachimine K, Abe H et al (2007) Sonodynamic therapy of cancer using novel sonosensitizers. Anticancer Res 27:3673–3677

Marchioni C, Riccardi E, Spinelli S, Dell'Unto F, Grimaldi P, Bedini A, Giliberti C, Giuliani L, Palomba R, Congiu Castellano A (2009) Structural changes induced in proteins by therapeutic ultrasounds. Ultrasonics 49:569–576

Pozzi D, Grimaldi P, Gaudenzi S, Di Giambattista L, Silvestri I, Morrone S, Congiu Castellano A (2007) UVB-radiation-induced apoptosis in jurkat cells: a coordinated fourier transform infrared spectroscopy-flow cytometry study. Rad Res 168:698–705

Rosenthal I, Sostaric JZ, Riesz P (2004) Sonodynamic therapy—a review of the synergistic effects of drugs and ultrasound. Ultrasound Sonochem 11:349–363

Shohet RV, Chen S, Zhou YT, Wang Z, Meidell RS, Unger RH, Grayburn PA (2000) Echocardiographic destruction of albumin microbubbles directs gene delivery to the myocardium. Circulation 101:2554–2556

Strom-Jensen PR, Dunn F (1984) Ultrasonic absorption by solvent–solute interaction and proton transfer in aqueous solutions of peptides and small proteins. J Acoust Soc Am 75:960–966

Wang JF, Wu CJ, Zhang CM, Qiu QY, Zheng M (2009) Ultrasound-mediated microbubble destruction facilitates gene transfection in rat C6 glioma cells. Mol Biol Rep 36:1263–1267

Wang J, Guo Y, Gao J, Jin X, Wang Z, Wang B, Li K, Li Y (2010) Detection and comparison of reactive oxygen species (ROS) generated by chlorophyllin metal (Fe, Mg and Cu) complexes under ultrasonic and visible-light irradiation. Ultrasound sonochem 18(5):1028–1034. doi:10.1016/j.ultsonch.2010.12.006

Xiang J, Xia X, Jiang Y, Leung AW, Wang X, Xu J, Wang P, Yu H, Bai D, Xu C (2010) Apoptosis of ovarian cancer cells induced by methylene blue-mediated sonodynamic action. Ultrasonics 51:390–395

Yow CM, Wong CK, Huang Z, Ho RJ (2007) Study of the efficacy and mechanism of ALA-mediated photodynamic therapy on human hepatocellular carcinoma cell. Liver Int 27:201–208